ELSEVIER Solar Energy Materials & Solar Cells 57 (1999) 153–165

Solar Energy Materials & Solar Cells

The role of the buffer layer in the light of a new equivalent circuit for amorphous silicon solar cells

J. Merten*, C. Voz, A. Muñoz, J.M. Asensi, J. Andreu

Departament de Física Aplicada i Òptica, Universitat de Barcelona, Av. Diagonal 647, E-08028 Barcelona, Spain

Abstract

Although the beneficial effect of the buffer layer between the p- and i-layer of amorphous silicon solar cells has been known for many years, the role of this layer is controversial. This paper examines the effect of the buffer layer using a new equivalent circuit for these devices (Merten et al. IEEE Trans. Electron Dev. 45 (1988) 423–429 [1]). The parameters of this model can be easily assessed by variable illumination measurements (VIM) of the devices' $I(V)$-curve. With the model, collection of carriers in the bulk of the cell is easy and clearly separated from the diode behaviour of the device. The VIM-method allows for a complete analysis of the thin film cells, covering both technological and physical topics. It is shown that the dominant effect increasing the efficiency of the cells with buffer layer is the reduction of the hole injection from the p-layer which leads to a reduced diode term. The buffer layer only slightly reduces the recombination in the i-layer. This reduction mainly occurs in a region close to the p/i-interface and cannot be observed with red light (homogeneous carrier generation).

Keywords: Buffer layer; Amorphous silicon solar cells; Open-circuit voltage; Short-circuit resistance

1. Introduction

It is widely accepted that buffer layers between the p- and the i-layer increase the efficiency of amorphous silicon solar cells [2–6]. The main effect observed is an

* Corresponding author. E-mail: jmerten@fao.ub.es

0927-0248/99/$ – See front matter
PII: S0927-0248(98)00169-X

increase in the open-circuit voltage V_{oc} of the cells, and better fill factors [6–8]. However, no more specific details can be obtained from these single $I(V)$-measurements. In particular, no detailed information can be obtained about the role of the buffer layer.

We therefore propose to perform varying illumination level measurements (VIM) on these devices and to obtain $I(V)$-curves for a whole set of illumination levels. The characteristic parameters of these $I(V)$-curves can be interpreted by a novel model for amorphous silicon solar cells. Although this model has been developed under the assumption of homogeneous carrier generation in the device, it fits the experimental data for white light illumination levels that vary over more than six orders of magnitude [1]. The VIM-data interpreted by this model allow for an easy and precise separation between the influence of technological factors on the device performance and changes due to the Staebler–Wronski effect [1,9]. The interpretation of this model also allows for a separate assessment of the device's rectifying quality and i-layer recombination. A very similar model has also been applied to microcrystalline silicon (μc-Si : H) thin film solar cells with pin structure [10].

We compare VIM-data of cells with and without buffer layer, which are furthermore obtained under blue and red light illumination. The resulting data are discussed in the light of the model. In this way, changes in the carrier generation profile give us a closer insight into the role of the buffer layer in amorphous silicon solar cell and modules.

2. Experimental methods

2.1. The cells examined

The cells were deposited in the same run using a monochamber glow discharge reactor without load-lock described in Ref. [11]. As the p-, i- and n-layer of the cells were simultaneously deposited; these layers had the same material properties for all the cells presented in this article. The buffer layer thickness $d_{p/i} = 0$, 2, 4 and 6 nm was controlled by a shutter. The thickness of the p-layer is 8 nm, of the i-layer is 450 nm and of the n-layer is 27 nm.

2.2. The measurements

The VIM method consists of the measurement and interpretation of the $I(V)$-curve parameters under logarithmically varying illumination levels. The variation of the illumination level is achieved by using neutral grey filters, not by changing the lamp current, in order to ensure similar illumination spectra. The illumination source was a halogen lamp driven by a constant DC current. Care was taken to illuminate only an area which is completely covered by the metal back contact of the cell (0.25 cm^2). The measured $I(V)$-curves are condensed into six characteristic parameters, which are:

1. the short-circuit current I_{sc};
2. the open-circuit voltage V_{oc};

3. the fill factor FF;
4. the efficiency η;
5. the *open-circuit resistance* ($R_{oc} = \partial V/\partial I)_{I=0}$, which may be related to the series resistance R_s of the cell, and
6. the *short-circuit resistance* ($R_{sc} = \partial V/\partial I)_{V=0}$, which may be related to the parallel resistance R_p of the cell.

These parameters are represented as a function of the short-circuit current, which serves as a measure of the illumination level. In this article, only open-circuit voltage and short-circuit resistance data are examined, the first to assess the rectifying quality of the device, the second to assess recombination losses in the i-layer of the cell.

White light or filtered light with coloured filters (blue or red) was used in order to vary the carrier generation profile in the cells. Fig. 1 shows the transmission spectra of the filters used. The use of the red filter leads to a homogeneous carrier generation throughout the cell, whereas the blue light generates carriers in the first 0.1 μm of the cell.

2.3. The model

The model used to evaluate the VIM-data is shown in Fig. 2. It consists of a single exponential term, which is supplemented by an additional term representing the recombination losses in the i-layer of the device. Series (R_s) and parallel (R_p) resistances are included to take into account technological issues such as TCO-conductivity and pin holes. This model is developed from the crude assumption of

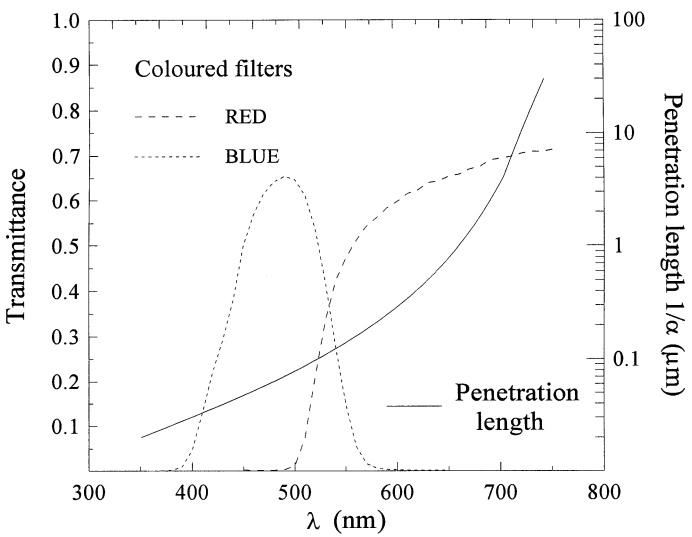

Fig. 1. The transmission spectra of the colour filters used. The solid line shows the measured absorption length of the i-layer material.

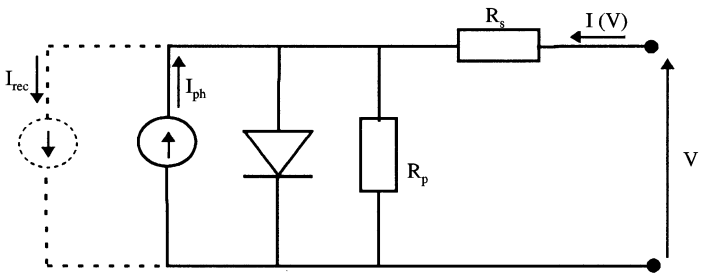

Fig. 2. The equivalent circuit of the model. The current sink I_{rec} stands for recombination losses in the i-layer.

homogeneous carrier generation and constant electrical field in the i-layer of the device. This is more likely for cells with a low defect density i-layers and low external voltages (i.e. in the short-circuit region). This model fits the experimental data for illumination levels covering more than six orders of magnitude [1]:

$$I(V) = -I_{ph} + I_{ph}\frac{d_i^2}{\mu\tau_{eff}\cdot[V_{bi}-(V-IR_s)]} + I_0\left(e^{\frac{V-IR_s}{nkT/e}}-1\right) + \frac{V-IR_s}{R_p}. \quad (1)$$

I_{ph} is the photogenerated current, I_0 the diode saturation current, n the diode quality factor, e is the elementary charge, k Boltzmanns' constant and T the temperature of the device. Apart from the parasitic resistances, the diode and the recombination in the i-layer represent the collection losses within the model.

The recombination losses in the i-layer are represented by the second term on the right-hand side of Eq. (1); this term, introduced in Ref. [1], is indicated by the current sink drawn with dashed lines in Fig. 2. It contains the intrinsic layer thickness d_i and an effective $\mu\tau$-product $\mu\tau_{eff}$ that quantifies the quality of the active layer in terms of recombination of photogenerated carriers.

The role of the diode term is the subject of the discussion in Section 4. Here we only draw attention to the fact that this simple model implies the validity of the superposition principle for the pin junction (i.e. neglecting the parasitic series resistance). Of course, it is clear that the electrical field in the device is not independent of illumination, which can be seen from the simple fact that the diode saturation current I_0 in the dark is very different from I_0 under illumination. However, the experimental behaviour of the cells is quite well described by the model. We therefore use this model to examine the effects of the buffer layer on the two principle loss terms of the model and thereby come to a deeper understanding of the role of these loss terms.

3. The physics of the main loss terms

The model has been shown to fit the data of amorphous silicon solar cells for illumination levels covering more than six orders of magnitude [1]. The suitability of the model can be seen from the VIM-data shown in Fig. 3a and Fig. 4a for a cell with

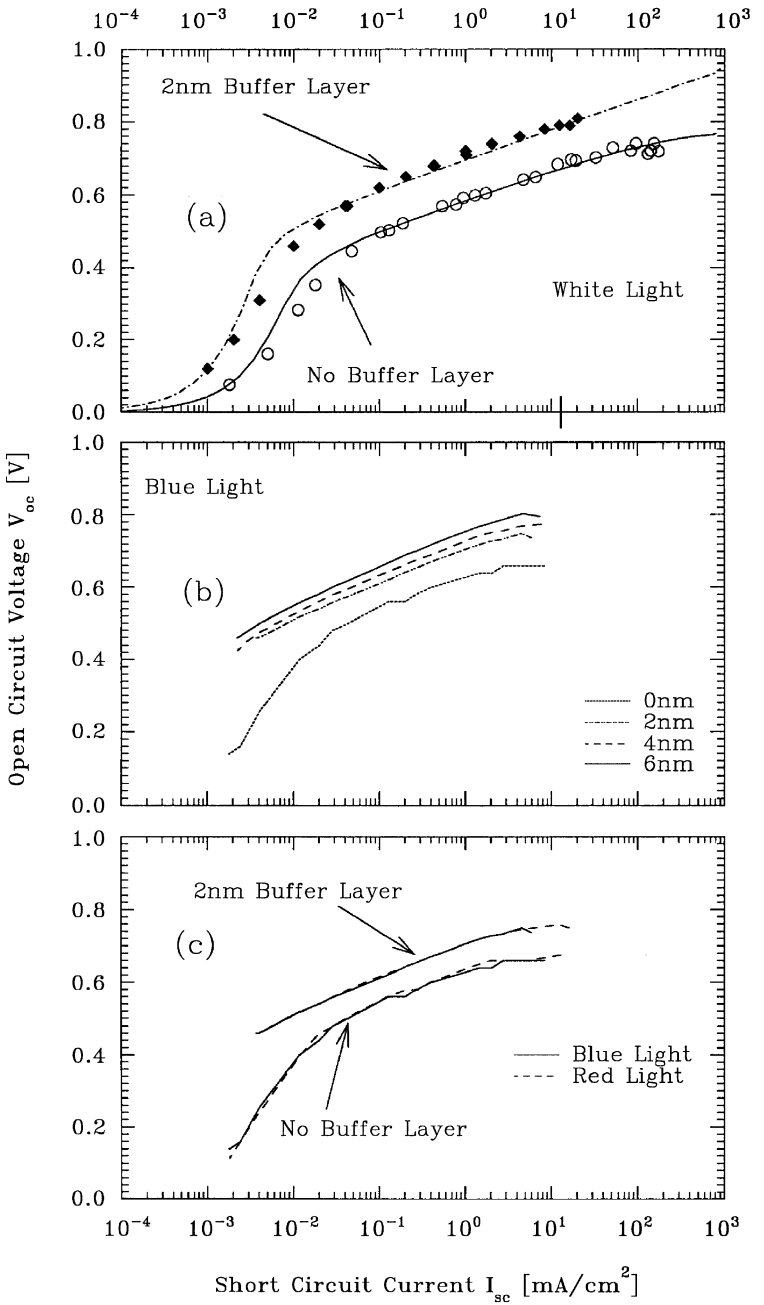

Fig. 3. The open-circuit voltage V_{oc} of the cell series (a) under white light illumination, (b) as function of the buffer layer thickness $d_{p/i}$ and (c) as a function of the illumination spectra. V_{oc} increases with $d_{p/i}$ (indicated in the legend) and does not depend on the illumination spectra.

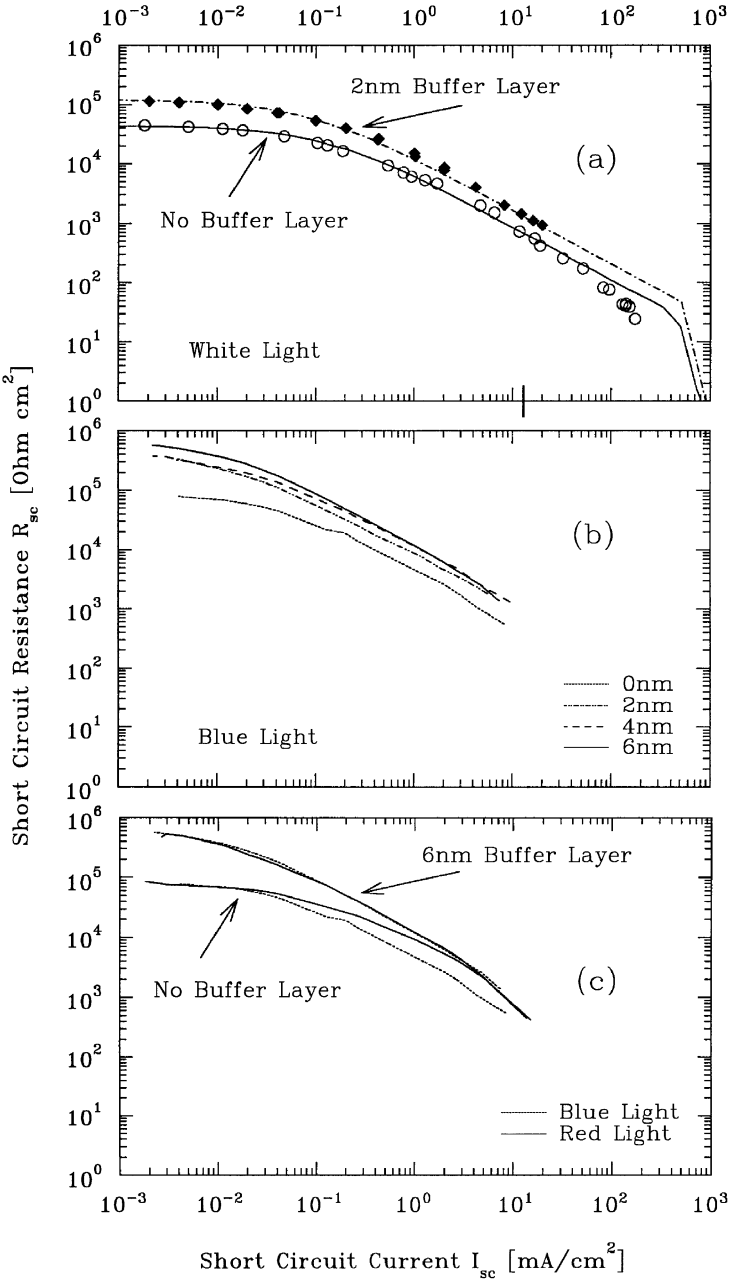

Fig. 4. The short-circuit resistance R_{sc} of the cell series (a) under white light illumination, (b) as function of the buffer layer thickness $d_{p/i}$ and (c) as a function of the illumination spectra. R_{sc} increases with $d_{p/i}$ (indicated in the legend), but saturates. For $d_{p/i} = 6$ nm, R_{sc} does not depend on the illumination spectra, for $d_{p/i} = 0$ nm, it does. For red light illumination, R_{sc} of the cells with and without buffer layer is the same (c).

and without buffer layer under white light illumination. The table shows the modelled parameters for these two cells. We now discuss the physics behind the main loss terms of the model and examine the role of the buffer layer.

The VIM-data presented in Fig. 3a and Fig. 4a were obtained under white light illumination. Closer insights into the role of the buffer layer can be obtained from the additional variation of the carrier generation profile in the cell. Before starting the discussion, however, we shall briefly examine the parasitic parallel resistance of the cells, because it affects our measurements.

3.1. The parallel resistance R_p

According to the model, the short-circuit resistance R_{sc} for lowest illumination levels equals the parallel resistance R_p of the device. This can be seen in Fig. 4, where R_{sc} of the cell without buffer layer is constant for low illumination levels represented by short-circuit currents below 10^{-2} mA/cm^2 (illumination regime A and B in Ref. [1]). This indicates that the cell without buffer layer has a higher pinhole density than the cells with buffer layer. The pinhole density, however, also depends on the history of the sample, for example, the mechanical stress suffered or the thermal treatments undergone. So the data in Fig. 4a indicate lower values for the parallel resistance R_p of the cells than Fig. 4b. This has nothing to do with the change of the illumination spectra, but with the fact that the data from Fig. 4b are older than the data in Fig. 4a. Between the measurements, the cells have undergone an additional 2 hours annealing at 150°C in order to assure them to have the same state of degradation. This anneal improved the parallel resistance R_p of the cells both with and without buffer layer. We also found that the parallel resistance R_p of our cells varies from contact to contact.

The parallel resistance R_p of the cell without buffer layer is lower than R_p of the other cells. However, one cannot draw further conclusions from this result as this would require a statistical treatment of data coming from many samples.

In what follows, it is important to note that, if we want to use R_{sc} for the assessment of the recombination in the i-layer of the device, we have to avoid the region where R_{sc} is independent of the illumination level, because in this regime R_{sc} equals the parallel resistance R_p.

3.2. The diode term: Carrier injection or interface recombination?

The parameters of the diode term of the model are assessed from the $V_{oc}(I_{sc})$ behaviour as shown in Fig. 3a for white light. The relation between V_{oc} and I_{sc} according to the model in Eq. (1) can be expressed as

$$V_{oc} = \frac{nkT}{e} \ln\left(\frac{I_{sc}}{I_0}\right). \tag{2}$$

This expression is valid for high illumination levels but not for low-level illumination where the parallel resistance governs the open-circuit voltage ($V_{oc} = R_p I_{sc}$, Regime A in Ref. [1]). A more important assumption leading to Eq. (2) is to neglect the

voltage dependence of the term representing the i-layer bulk recombination losses (second term on the right-hand side of Eq. (1)). The calculations of the model with parameters which fit the experimental data for thin amorphous silicon solar cells (0.3 μm) have shown that even for degraded cells, the i-layer recombination term has no effect on the open-circuit voltage of the device [1]. This finding is related to the strong dominance of the diode term in the open circuit region. The modelled V_{oc} is therefore not affected by the i-layer recombination term when the i-layer is thin enough to allow for an efficient photovoltaic operation of the device (i.e. 0.3 μm). The cells presented in this article are thicker (0.45 μm) and the i-layer recombination has a stronger effect and may affect the open-circuit voltage of the cells in the *degraded* state. However, using the parameters of the table, the modelled recombination loss term has no effect on the open-circuit voltage of the cell in the *annealed* state. We conclude that Eq. (2) is correct for the cells in the annealed state and that we can use the $V_{oc}(I_{sc})$-data to evaluate the diode term of the model.

The higher V_{oc} of the cells with buffer layer shown in Fig. 3 is modelled by a reduced diode saturation current I_0 (about one order of magnitude for white light illumination, Table 1). Dark $I(V)$ measurements confirm this tendency ([8], Table 1). This finding has been related to a reduction of the recombination at the p/i interface [8].

Some authors [6] state that, under illumination, the buffer layer increases the injection of carriers photogenerated in that layer into the i-layer and thus enhances the collection of carriers. However, no significant increase of the short circuit current could be detected for device where a buffer layer has been introduced [6].

Other authors [12] concluded from numerical simulations that the buffer layer reduces the recombination at the p/i interface, thus reducing I_0 and increasing V_{oc}, a statement that has found a wide acceptance among many authors [13]. However, Fig. 3c gives clear evidence that I_0 is not determined by the recombination at the p/i interface: the $V_{oc}(I_{sc})$-data do not depend on the illumination spectra. The modelled I_0 is independent of the carrier generation profile for cells both with and without buffer layer.

If the p/i interface recombination was to be critical for the open-circuit voltage, we would expect lower V_{oc} values in the case of blue light. The carriers generated close to the p/i interface would then recombine there and contribute to an increased diode saturation current I_0. It is clear from Fig. 3c that this is not the case and we conclude

Table 1
The parameters of the model used for the fitlines of Fig. 3a and Fig. 5a

Parameter	No buffer layer	2 nm buffer layer
V_{bi} (V)	1.1	1.1
$\mu\tau$ (cm^2/V)	1.4E-8	2.5E-8
I_0 (mA/cm^2)	7E-8	4E-9
n [1]	1.45	1.45
R_p ($k\Omega\,cm^2$)	44	120

that the p/i interface recombination has no effect on the modelled diode saturation current I_0 and no direct effect on the open-circuit voltage V_{oc}.

We propose that the modelled diode saturation current I_0 depends on the injection of the majority of carriers from the doped layers into the bulk of the device. The loss current modelled by the diode term is a pure property of the contacts i.e. the rectifying capacity of the device. It is clear that such a diode term does not depend on the illumination spectra (Fig. 3c). The improved open-circuit voltage of the cell with buffer layer is then explained by a reduction of the hole injection from the p-layer, an effect that increased with the thickness of the buffer layer (Fig. 3b).

We conclude that the buffer layer reduces the injection of holes from the p-layer into the i-layer and that this is the effect that improves the open-circuit voltage of the device.

3.3. The i-layer recombination term

The recombination in the i-layer of the device is modelled by the second term on the right-hand side of Eq. (1), which is also shown by dashed lines in Fig. 2. According to this model, the slope R_{sc} is determined exclusively by the bulk recombination term when the illumination level is high enough for R_{sc} not to be affected by the parallel resistance and low enough for R_{sc} not to be affected by the series resistance R_s (regime C and D in Ref. [1]):

$$R_{sc} = \frac{1}{I_{ph}} \cdot \mu\tau_{eff} \cdot \frac{V_{bi}^2}{d_i^2}. \tag{3}$$

Assuming similar values for V_{bi} and d_i, we can assess with R_{sc} the recombination in the i-layer of the device: high values for R_{sc} stand for low recombination in the bulk of the cells and hence for efficient carrier collection. Thus, R_{sc} is a powerful tool to assess $\mu\tau_{eff}$, a feature that has been already used for the long-term monitoring of the state of Staebler–Wronski degradation of a commercial amorphous silicon module [14].

Eq. (3) is deduced from the model that is based on the assumption of homogeneous carrier generation and homogeneous electrical field in the device. The model fits well to the $R_{sc}(I_{sc})$ data shown in Fig. 4a and we may use R_{sc} to assess the recombination in the i-layer of the cells presented in this article. However, we will not use R_{sc} for quantitative statements here, but for qualitative comparisons in order to elucidate the role of the buffer layer for the i-layer recombination. In conclusion, increased values for R_{sc} stand for reduced recombination in the i-layer and better carrier collection.

Fig. 4a shows that R_{sc} of the cell with buffer layer is increased for white light. This indicates that the buffer layer improves the collection of carriers and the buffer layer indeed reduces the recombination in the i-layer of the cell.

Fig. 4b shows the dependence of $R_{sc}(I_{sc})$ on the buffer layer thickness $d_{p/i}$ measured with blue light illumination. In the regime, where R_{sc} is not affected by the parallel resistance of the devices, R_{sc} increases with the thickness of the buffer layer. For sufficiently thick buffer layers (4 nm), however, this effect saturates and no more R_{sc} can be gained for the cell with the 6 nm buffer layer.

The data shown here come from cells in the annealed state. As they were all deposited in the same run and they all underwent the same annealing procedure, we may assume the $\mu\tau$-product of the i-layer material to be the same for all the cells examined.

The data shown in Fig. 4 therefore indicate that carriers generated in the region close to the p-layer of the device are better collected when there is a buffer layer. The recombination in the i-layer for these carriers is reduced with the presence of the buffer layer. Once the buffer layer is thick enough, no further reduction of the bulk recombination can be obtained.

In this regime (i.e. thick buffer layers), the $R_{sc}(I_{sc})$ data do not depend on the illumination spectra (Fig. 4c). Bulk recombination losses are the same for red and blue light illumination in the case of the cell with the thickest buffer layer. Although carriers generated by blue light are exposed closer to the p/i-interface region, they do not suffer more recombination losses than homogeneously generated carriers. This indicates that the thick 6 nm buffer layer efficiently reduces the bulk recombination in the p/i-interface region.

For the cell without buffer layer, however, Fig. 4c shows that R_{sc} under red light is higher than with blue light. This indicates that there is a pronounced recombination in the bulk of the cell in a region close to the p/i-interface. This recombination has less weight when the carriers are generated homogeneously over all the thickness of the device, as is the case with red light. For homogeneous carrier generation, the bulk recombination in the p/i-interface region can be neglected.

On the basis of the foregoing, it is no surprise that the R_{sc}-data under red light illumination of the cell without buffer layer coincide with the data of the cell with 6 nm buffer layer. This can be observed in Fig. 4c for an illumination range, in which R_{sc} is not affected by the parallel resistance ($I_{sc} > 1$ mA/cm^2). (The slight reduction of the R_{sc}-data visible in Fig. 4b for currents of more than 10 mA/cm^2 is caused by the series resistance of the cells.)

Concluding, the buffer layer does not improve the collection of all carriers generated in the i-layer of the device, but of carriers generated close to the p/i-interface. That is why the buffer layer improves R_{sc} measured with white light, but not R_{sc} measured with red light.

4. Buffer layer and V_{oc} engineering

It has been shown in the last section that the buffer layer reduces the majority carrier injection of the p-layer and that this effect is stronger for thicker buffer layers. Furthermore, i-layer recombination could be slightly reduced with the buffer layer. This would mean that the thickest buffer layers are best for the device performance.

However, thicker buffer layers increase the inverse slope R_{oc} and decrease the fill factor of the cells (Fig. 1d). Further research is called for to clearly understand this behaviour. In any case, the detrimental effect of thicker buffer layers on the fill factor requires a reduction of the buffer layer thickness to the minimum possible value.

For the optimisation of the open-circuit voltage, one has to understand which loss term of the model limits the open-circuit voltage. The simplest case would be presented by a "shunted cell", that is a device with such a low parallel resistance that the shunt current becomes the most important loss of the device. The higher the illumination level, the less critical this issue becomes. However, this issue may become important in the case of operation under indoor conditions with low illumination.

The open-circuit voltage of non-shunted devices may be limited by the diode term or the recombination term of the model. For solar cells with the usual thickness of 0.3 μm, it has been shown in Ref. [1] that it is the diode term that governs the open-circuit voltage, even in the case of the degraded cell.

The cells examined in this article are thicker. The calculations of the model (with the parameters from Table 1) have shown that, in the case of the annealed cells, the effect of the recombination term on the open-circuit voltage is minimal. Thus, it is the diode term that governs the open-circuit voltage. This fact was a prerequisite for the discussion in Section 3.2.

The losses of the diode term can be reduced with the buffer layer, and thicker buffer layers further reduce the diode term. As this is the term that governs V_{oc}, the values for V_{oc} shown in Fig. 5a increase with the buffer layer thickness.

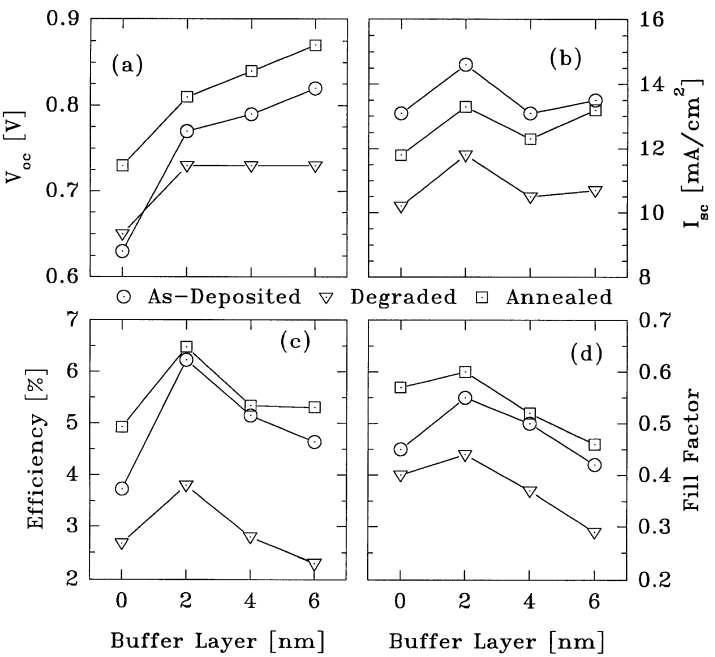

Fig. 5. Solar cell parameters in the as-deposited state, after 72 days outdoor degradation and after annealing as a function of the buffer layer thickness $d_{p/i}$. The short-circuit current I_{sc} shown in this figure has been normalized to 1 sun illumination (100 mW/cm^2). Variations of I_{sc} are attributed to thickness variations of the i-layer. The data shown have been obtained outdoors around noon under clear irradiance conditions. The optimum value for $d_{p/i}$ is 2 nm.

For the "thick" degraded cells shown by the triangles in Fig. 1a the situation is different. The buffer layer reduces the diode term, and the "bad" V_{oc} of the cell without the buffer layer is improved by about 0.07 V. However, a further increase in the buffer layer thickness has no positive effect on V_{oc} of the degraded cells, because now it is the i-layer recombination that governs the open-circuit voltage.

In the case of commercial application of amorphous silicon solar cells and modules, it is clear that the optimum buffer layer thickness should be determined for a *degraded* device. For the thick cells examined here, the optimum thickness was 2 nm (Fig. 5c). In general, the positive effect of thick buffer layers on the open-circuit voltage is destroyed by the worse fill factor. The optimum value found here is for orientation only, as it may change with the details of the deposition conditions, doping levels, and, of course, with the thickness of the cells.

5. Conclusions

Variable illumination measurements (VIM) of the $I(V)$ characteristic of amorphous silicon solar cells provide insight into the physics of these devices, especially when these measurements are performed with changing illumination spectra. The VIM-data are interpreted by a novel model for amorphous silicon solar cells and modules which, apart from parasitic resistances, consist of a current source, a diode term and an additional term taking into account recombination losses in the i-layer of the device.

It is shown that the model allows for a separate assessment of the effects concerning parallel resistance, diode term and i-layer recombination. This allowed for a closer insight into the role of the buffer layer of amorphous silicon solar cells.

The diode term of this model is determined by the majority carrier injection of the doped layers and not by recombination at the p/i-interface. The reduction of the diode term (i.e. the improvement of the open-circuit voltage) with the buffer layer should therefore be attributed to modifications of the injection conditions for holes from the p-layer and not to a reduction of recombination at the p/i-interface.

The belief that buffer layers reduce the recombination at the p/i-interface is, however, confirmed. This finding is modelled with an increase of the newly introduced term representing the recombination losses in the i-layer of the device. The effect of this improvement, however, does not increase the open-circuit voltage of the device and becomes negligible in the case of homogeneous carrier generation.

As the strong i-layer recombination governs the open-circuit voltage of the thick degraded cells with buffer layer, no further V_{oc} can be gained by making this layer thicker than 2 nm. As thicker buffer layers reduce the fill factor of the cells, there is an optimum thickness for the buffer layer, which may be higher for thinner cells.

Acknowledgements

This work was supported by the DGICYT of the Spanish Government (TIC98-0381-C02-01) and Generalitat de Catalunya.

References

[1] J. Merten, J.M. Asensi, C. Voz, A.V. Shah, R. Platz, J. Andreu, IEEE Trans. Electron Dev. 45 (1988) 423.
[2] B. Samanta, Debarata Das, A.K. Barua, Sol. Energy Mater. Sol. Cells 46 (1997) 233.
[3] H. Tanaka, N. Ishiguro, T. Miyashita, N. Yanagawa, M. Sadamoto, M. Koyama, Y. Ashida, N. Fukuda, Sol. Energy Mater. Sol. Cells 34 (1-4) (1994) 493.
[4] Y. Ashida, Sol. Energy Mater. Sol. Cells 34 (1-4) (1994) 291.
[5] Y. Arai, M. Ishii, H. Shinohara, S. Yamazaki, IEEE Electron Dev. Lett. 12 (1991) 460.
[6] P. Chaudhuri, S. Ray, A.K. Batabyal, A.K. Barua, Sol. Energy Mater. Sol. Cells 36 (1995) 45.
[7] W. Kusian, H. Pfleiderer, W. Jürgens, Buffer Layer and Light degradation of a-Si PIN Solar Cells, Proc. 9th E.C. Photovoltaic Solar Energy Conf. 1989, pp. 52–55.
[8] H. Sakai, T. Yoshida, S. Fujikake, T. Hama, Y. Ichikawa, J. Appl. Phys. 67 (1990) 3494.
[9] J. Merten, J.M. Asensi, J. Andreu, A.V. Shah, Assesing Amorphous Silicon Solar Modules by Variable Illumination Measurements (VIM) of the I(V)-Characteristic, In: Proc. 14th European Photovoltaic Conf., Barcelona 1997, pp. 260–263.
[10] J. Merten, A. Muñoz, C. Voz, J. Andreu, H. Meier, P. Torres, A.V. Shah, Variable Illumination Measurements of Microcrystalline Silicon Solar Cells, In: Proc. 14th European Photovoltaic Conf., Barcelona 1997, pp. 1424–1427.
[11] J. Bertomeu, J.M. Asensi, J. Puigdollers, J. Andreu, J.L. Morenza, Vacuum 44 (1993) 129.
[12] S. Yamanaka, M. Konagai, K. Takahashi, Japanese J. Phys. 28 (7) (1989) 1178.
[13] W. Kusian, H. Pfleiderer, J. of Non Cryst. Solids 164–166 (1993) 713.
[14] J. Merten, J. Andreu, Clear separation of seasonal effects on the performance of amorphous silicon solar modules by outdoor I/V-measurements, Sol. Energy Mater. Sol. Cells, accepted.